Supporting Information

Isomerization enabling near-infrared electron acceptors

Jiasi Luo, [a†], Yang Wang, *[a†] Bin Liu, [a] Ziang Wu, [b] Yujie Zhang, [a] Yumin Tang, [a] Peng Chen, [a] Qiaogan Liao, [a] Han Young Woo, [b] Xugang Guo *[a]

[a] Department of Materials Science and Engineering and The Shenzhen Key Laboratory for Printed Organic Electronics, Southern University of Science and Technology (SUSTech), No. 1088, Xueyuan Road, Shenzhen, Guangdong 518055, China. Email: wangy6@sustech.edu.cn; guoxg@sustech.edu.cn

[b] Department of Chemistry, Korea University, Seoul 02841, South Korea.

† These authors contributed equally to this work.

ORCID:

Yang Wang: 0000-0002-3669-0192

Xugang Guo: 0000-0001-6193-637X

Han Young Woo: 0000-0001-5650-7482

1. Materials and Instruments.

All reagents and chemicals are commercially available and are used without further purification unless otherwise stated, among which the donor polymer PBDB-T (made by 1-Material) was purchased from J&K Scientific LTD (China). Anhydrous toluene and tetrahydrofuran (THF) were distilled from Na/benzophenone under argon flow. All reactions were carried out under inert atmosphere unless otherwise stated. The ^{1}H NMR and ^{13}C NMR spectra were measured on the Bruker Ascend 400 MHz spectrometer. High-resolution mass spectra were obtained with ThermoScientific™ Q-Exactive. Elemental analyses (EAs) of compounds were performed at Shenzhen University (Shenzhen, Guangdong, China). UV-vis optical absorption spectra of solutions and thin films were recorded on a Shimadzu UV-3600 UV-VIS-NIR spectrophotometer. Cyclic voltammetry measurements were carried out under argon atmosphere using the CHI760E voltammetric workstation with a N_2-saturated solution of 0.1 M tetra-n-butyl ammonium hexafluoro phosphate (Bu_4NPF_6) in acetonitrile (CH_3CN) as the supporting electrolyte. A platinum disk working electrode, a platinum wire counter electrode, and a silver wire reference electrode were employed, and the ferrocene/ferrocenium redox couple (Fc/Fc^+) was used as the reference for all measurements with a scanning rate of 50 mV s^{-1}. Atomic Force Microscopy (AFM) measurements were conducted using a Dimension Icon Scanning Probe Microscope (Asylum Research, MFP-3D-Stand Alone) in the tapping mode. 2D GIWAXS measurements were carried out at the PLS-II 9A U-SAXS beam line of Pohang Accelerator Laboratory, Korea.

2. Fabrication and characterization of organic photovoltaics

OPVs were fabricated in the configuration of the traditional sandwich structure with an indium tin oxide (ITO) glass (12 Ω sq^{-1}) positive electrode and a PDINO/Al negative electrode. The ITO glass was pre-cleaned in an ultrasonic bath of detergent, deionized water, acetone, and isopropanol, and UV-treated in ultraviolet-ozone chamber for 15min. A thin layer of PEDOT:PSS (poly(3,4-ethylene dioxythiophene): poly(styrene sulfonate)) (Clevios P VP A1 4083) was prepared by spin-coating the PEDOT:PSS solution filtered through a 0.45 mm poly(tetrafluoroethylene) (PTFE) filter at 2,700 rpm for 30 s on the ITO substrate. Subsequently, PEDOT:PSS film was

baked at 150℃ for 15 min in the air, and the thickness of the PEDOT:PSS layer was about 35 nm. The blend solution PBDB-T: DTA-IC-S (D:A = 1:1.5, 12 mg mL^{-1} in total) or PBDB-T:DTA-IC-M (D:A = 1:1, 14 mg mL^{-1} in total) was dissolved in chlorobenzene (CB) and spin-cast at 1,000 rpm for 40 s onto the PEDOT:PSS layer. The thickness of the photoactive layer for DTA-IC-S and DTA-IC-M are about 120 nm and 100 nm, respectively, measured by Ambios Technology XP-2 profilometer. Before spin-coating the electron transporting layer, all active layers were thermally annealed at 100 ℃ for 10 min. Subsequently, 5 nm of the perylene diimide functionalized with amino N-oxide (PDINO) (1.5 mg mL^{-1} in ethanol) was spin-coated at 3000 rpm for 27 s on the active layer. Finally, 100 nm Al cathode were deposited in a vacuum onto the electron transporting layer under a high vacuum (3E−6 Torr) using thermal evaporation.

The *J-V* curves were measured on a computer-controlled Keithley 2400 source meter under 1 sun, the AM 1.5 G spectra came from a class Xe lamp-based SS-F5-3A solar simulator (Enli Technology, Inc.), and the light intensity was 100 mWcm^{-2} as calibrated by a an NREL-calibrated Si solar cell with a KG-5 filter. The external quantum efficiency (EQE) was measured by a QE-R3011 measurement system (Enli Technology, Inc.). A calibrated silicon detector was used to determine the absolute photosensitivity at different wavelengths. All of these fabrications and characterizations were conducted in a glove box.

3. Mobility measurements

The hole-only or electron-only diodes were fabricated using the following architectures: ITO/PEDOT: PSS/active layer/Ag for holes and ITO/ZnO/active layer/PDINO/Al for electrons. Mobilities were extracted by fitting the current density voltage curves using the space charge limited current (SCLC) method. The mobilities were obtained by taking current-voltage curves and fitting the results to a space

charge limited form. The SCLC mobilities were calculated based on the MOTT-Gurney equation:

$$J = \frac{9}{8}\varepsilon_0\varepsilon_r\mu\frac{V^2}{d^3}$$

Where J is the current density, ε_r is the relative dielectric constant of active layer material, usually 2-4 for organic semiconductors, herein we use a relative dielectric constant of 3 for polymer. ε_0 is the permittivity of empty space, μ is the mobility of hole or electron and d is the active layer thickness, V is the internal voltage in the device, and $V = V_{appl} - V_{bi}$, where V_{appl} is the voltage applied to the device, and V_{bi} is the built-in voltage resulting from the relative work function difference between the two electrodes (in the hole-only and the electron-only devices, the V_{bi} values can be neglected).

4. Morphology Characterization

The morphologies of the blend films were investigated by AFM (Asylum Research, MFP-3D-Stand Alone) in contacting under normal air conditions at room temperature. Samples for the TEM measurements were prepared as follows: the active layer films were spin-casted on ITO/PEDOT: PSS substrates, and the substrates with active layers were submerged in deionized water to make the active layers float onto the air-water interface. Then, the floated films were picked up on an unsupported 200 mesh copper grid for the TEM measurements.

5. Synthesis of DTA-IC-S and DTA-IC-M.

DTA-IC-S: It has been reported in our previous work[1].

Compound (1). This compound was synthesized according to the similar procedure described in our previous work[1]. Yield: 41%. Note that the solubility of the product is very poor. ^{1}H NMR (400 MHz, $C_2D_2Cl_4$) [ppm]: δ 7.80 (d, J = 5.3 Hz, 2H), 7.67-7.64 (m, 4H), 7.61 (d, J = 5.3 Hz, 2H), 7.40-7.38 (m, 4H), 3.48 (s, 6H).

Compound (2). This compound was synthesized according to the similar procedure described in our previous work[1]. Yield: 50%. ^{1}H NMR (400 MHz, $CDCl_3$) [ppm]: δ

9.07-9.05 (m, 2H), 7.55-7.52 (m, 2H), 7.36 (d, J = 5.2 Hz, 2H), 7.08 (br, 2H), 7.02 (d, J = 8.3 Hz, 8H), 6.93 (d, J = 8.2 Hz, 8H), 6.84 (d, J = 5.2 Hz, 2H), 2.56 (t, J = 7.6 Hz, 8H), 1.59-1.57 (m, 8H), 1.34-1.31 (m, 24H), 0.91-0.89 (m, 12H).

Compound (3). This compound was synthesized according to the similar procedure described in our previous work[1]. Yield: 80%. ^{1}H NMR (400 MHz, CDCl$_3$) [ppm]: δ 9.92 (s, 1H), 9.07-9.05 (m, 1H), 7.66-77.63 (m, 1H), 7.48 (s, 1H), 7.16-7.13 (m, 1H), 7.05 (d, J = 7.4 Hz, 1H), 6.89 (d, J = 7.2 Hz, 1H), 2.57 (t, J = 7.6 Hz, 8H), 1.59-1.56 (m, 8H), 1.35-1.32 (m, 24H), 0.90-0.88 (m, 12H).

DTA-IC-M: This compound was synthesized according to the similar procedure described in our previous work[1]. Yield: 66%. ^{1}H NMR (400 MHz, CDCl$_3$) [ppm]: δ 9.24-9.21 (m, 1H), 8.80 (s, 1H), 8.72 (d, J = 7.3 Hz, 1H), 7.97 (d, J = 6.3 Hz, 1H), 7.84-7.74 (m, 3H), 7.60 (s, 1H), 7.13 (s, 1H), 7.06 (d, J = 8.3 Hz, 4H), 6.89 (d, J = 8.3 Hz, 4H), 2.60-2.56 (m, 8H), 1.61-1.56 (m, 8H), 1.36-1.31 (m, 24H), 0.88 (t, J = 6.6 Hz, 12H). ^{13}C NMR (100MHz, CDCl$_3$): δ 188.14, 160.36, 149.78, 149.67, 145.87, 143.04, 141.88, 140.27, 140.02, 137.41, 137.29, 136.93, 135.18, 134.46, 129.58, 129.12, 128.86, 128.07, 127.03, 126.84, 126.68, 125.25, 123.86, 123.21, 114.65, 114.54, 69.46, 57.81, 35.46, 31.69, 31.19, 29.09, 22.57, 14.07. HRMS: C$_{98}$H$_{86}$N$_4$O$_2$S$_2$ calcd: 1414.6192, found: 1415.6137 [M+H]. Elemental Analysis: C, 83.13; H, 6.12; N, 3.96; S, 4.53, Found: C, 83.23; H, 6.01; N, 4.14; S, 4.39.
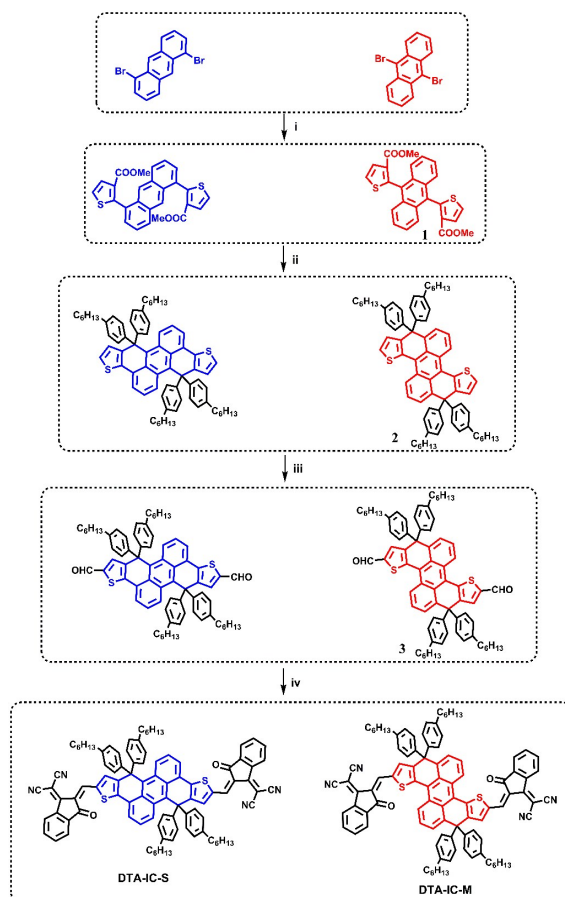
Scheme S1 Synthetic route for the compounds DTA-IC-S and DTA-IC-M.

Reagents and conditions: i) methyl 2-(trimethylstannyl)thiophene-3-carboxylate, Pd(PPh$_3$)$_4$, DMF, 110 ^{o}C; ii) 1-bromo-4-hexylbenzene, *n*-BuLi, -78 ^{o}C; then Amberlyst 15, toluene, reflux; iii) POCl$_3$, DMF, 1,2-dichloroethane, reflux; iv) 2-(1,2-dihydro-1-oxoinden-3-ylidene)malononitrile, pyridine, CHCl$_3$, reflux.
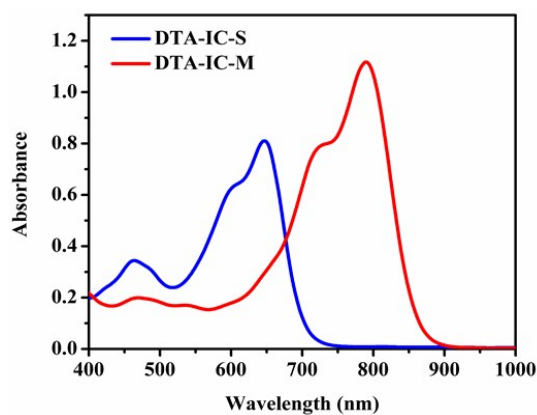

Figure S1 Absorption spectra of DTA-IC-S and DTA-IC-M in chloroform solutions with a concentration of 10^{-5} M.
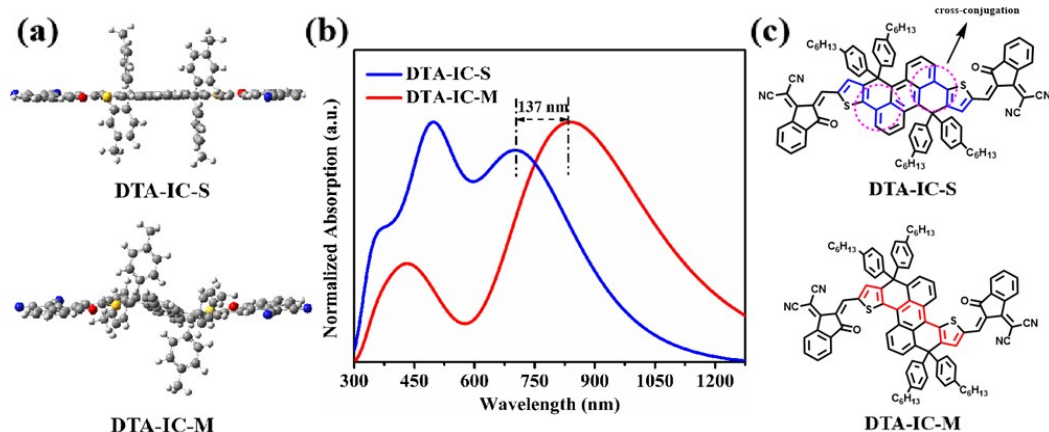
Figure S2 Optimized ground state molecular configurations for DTA-IC-S and DTA-IC-M (a), and the corresponding normalized absorption spectra from TD-DFT calculations (b) and chemical structures (c).

Table S1 The key electronic absorption spectra properties of DTA-IC-S and DTA-IC-M.

	Excited state	λ(nm)	Oscillator strength	Configuration
DTA-IC-S	S_1	702.28	1.1538	HOMO $\rightarrow$ LUMO (98%)
	S_6	501.86	1.1018	HOMO-1 $\rightarrow$ LUMO+1 (95%)
DTA-IC-M	S_1	840.28	1.6993	HOMO $\rightarrow$ LUMO (99%)
	S_{15}	415.14	0.2164	HOMO-1 $\rightarrow$ LUMO+1 (64%)
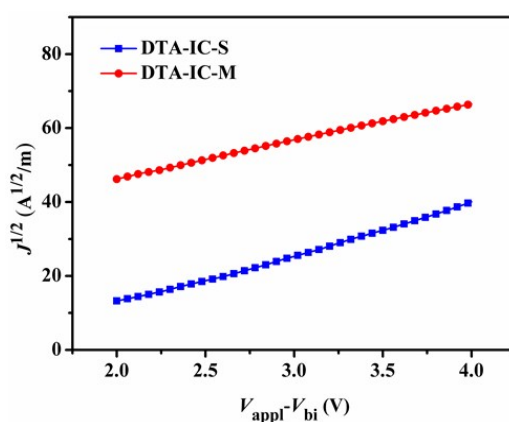
Figure S3 The corresponding $J^{1/2}$-V curves for electron-only devices based on the pure films of DTA-IC-S and DTA-IC-M (in dark).

Table S2 Optimal photovoltaic parameters of OPVs with different acceptors under optimized conditions and charge carriers mobilities by the SCLC model.

Active layer[a]	V_{oc}[b] (V)	J_{sc}[b] (mA/cm^2)	Cal. J_{sc}[c] (mA/cm^2)	FF[b] (%)	PCE[b] (%)	E_{loss}[d] (eV)	μ_h[e] (cm^2 V^{-1} s^{-1})	μ_e[e] (cm^2 V^{-1} s^{-1})	μ_h/μ_e
PBDB-T: DTA-IC-S	0.934±0.005 (0.938)	12.02±0.32 (12.27)	11.93	51.3±1.8 (52.9)	5.76±0.31 (6.09)	0.73	1.96×10^{-4}	2.96×10^{-5}	6.62
PBDB-T: DTA-IC-M	0.690±0.005 (0.693)	12.65±0.31 (12.96)	12.56	46.49±1.6 (46.78)	4.01±0.19 (4.20)	0.66	1.16×10^{-5}	9.37×10^{-5}	0.12

[a] With thermal annealing at 100 °C for 10 min. [b] Average values with standard deviation were obtained from 15 separate measurements and the values in parentheses are the parameters of the best devices. [c] J_{sc} integrated from EQE curve. [d] Energy loss. [e] Measured using a SCLC method.
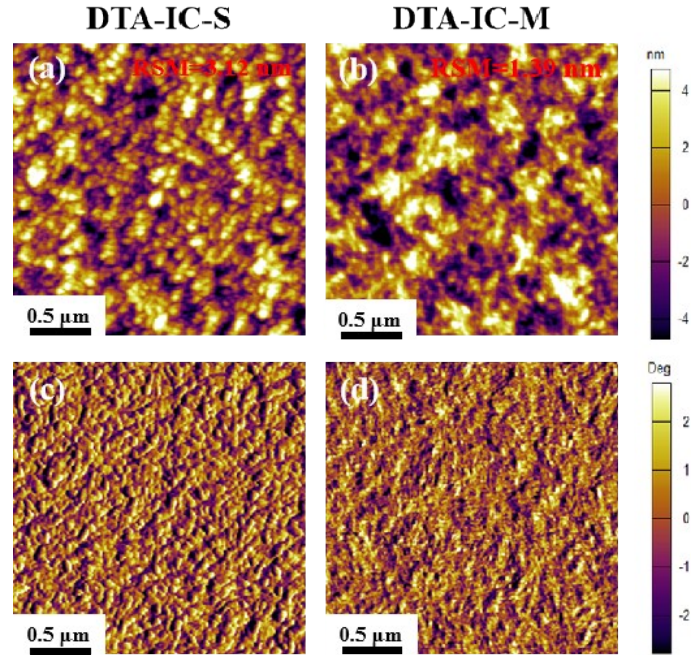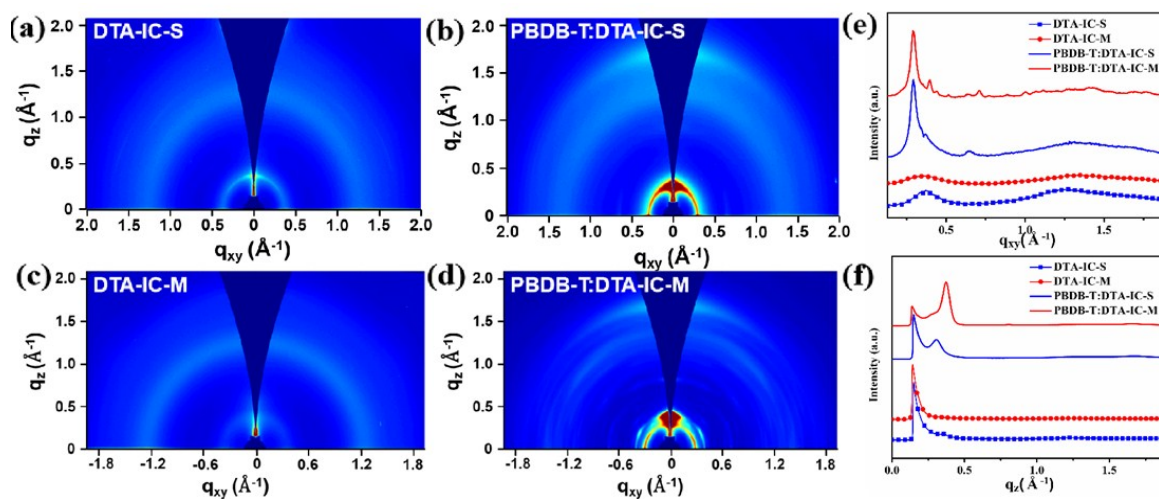

Figure S4 AFM height images of DTA-IC-S (a) and DTA-IC-M (b); the corresponding AFM phase images of DTA-IC-S (c) and DTA-IC-M (d).
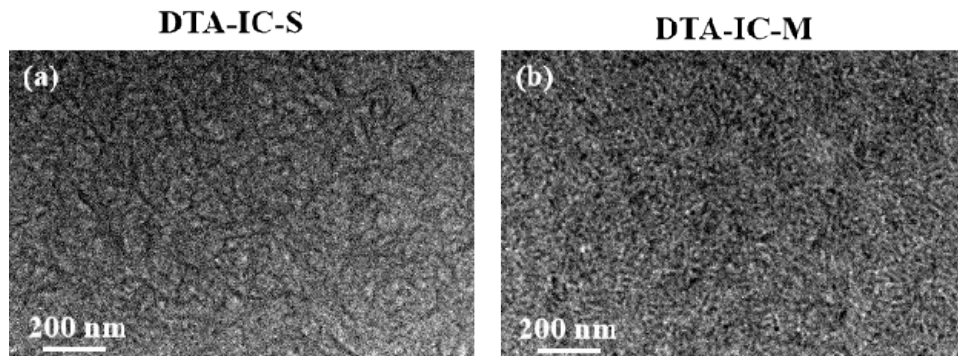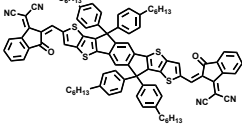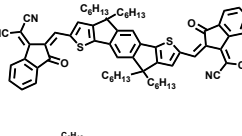
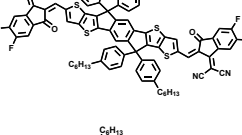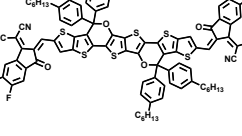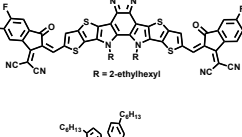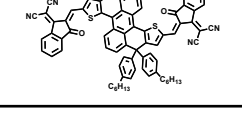**Figure S5** TEM images of PBDB-T: DTA-IC-S (a) and PBDB-T: DTA-IC-M (b) blend films.


Figure S6 Two-dimensional grazing-incidence wide-angle X-ray scattering (GIWAXS) patterns for pristine films of DTA-IC-S (a), DTA-IC-M (c) and blend films of PBDB-T:DTA-IC-S (b) and PBDB-T:DTA-IC-M (d); the corresponding line-cut profiles along the in-plane and out-of-plane directions (e, f).

Table S3. Comparison of DTA-IC-M with some benchmark nonfullerene acceptors.

Acceptor	Chemical Structure	ε (M^{-1} cm^{-1})	$\lambda_{max,film}$ (nm)	E_g (eV)	PCE (%)	Ref.
ITIC		1.3×10^5	702	1.59	6.80	[2]
IDIC		2.4×10^5	716	1.62	8.71	[3]
IT-4F		2.1×10^5	717	1.52	13.1	[4]
COi8DFIC		---	830	1.26	14.62	[5]
Y6		1.07×10^5	821	1.33	15.7	[6]
DTA-IC-M		2.23×10^5	822	1.35	4.20	This work
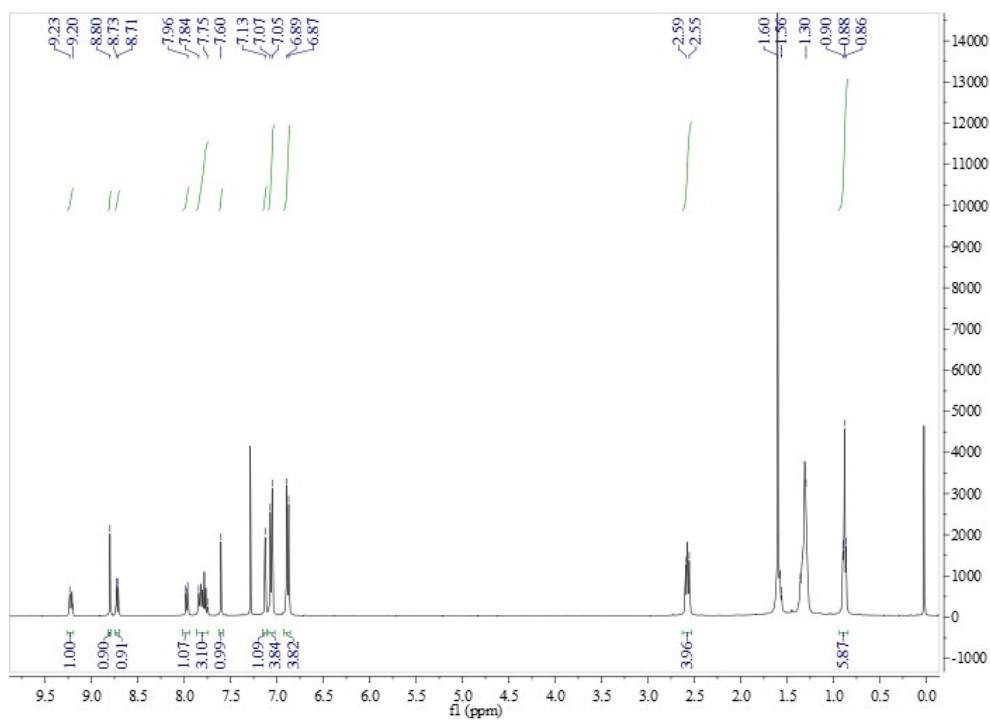
Figure S7 ¹H NMR spectrum of compound DTA-IC-M.
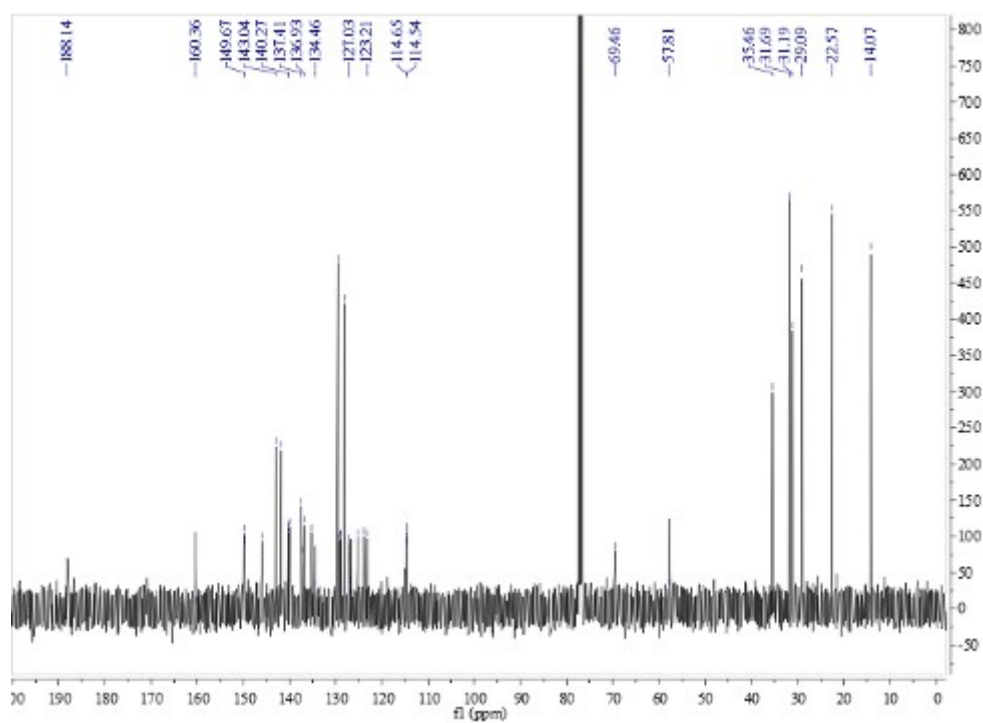
Figure S8 ¹³C NMR spectrum of compound DTA-IC-M.

References

1. Y. Wang, B. Liu, C. W. Koh, X. Zhou, H. Sun, J. Yu, K. Yang, H. Wang, Q. Liao, H. Y. Woo and X. Guo, *Adv. Energy Mater.*, 2019, **9**, 1803976.
2. Y. Lin, J. Wang, Z. Zhang, H. Bai, Y. Li, D. Zhu and X. Zhan, *Adv Mater*, 2015, **27**, 1170.
3. Y. Lin, Q. He, F. Zhao, L. Huo, J. Mai, X. Lu, C. J. Su, T. Li, J. Wang, J. Zhu, Y. Sun, C. Wang and X. Zhan, *J. Am. Chem. Soc.*, 2016, **138**, 2973.
4. W. Zhao, S. Li, H. Yao, S. Zhang, Y. Zhang, B. Yang and J. Hou, *J. Am. Chem. Soc.*, 2017, **139**, 7148.
5. Z. Xiao, X. Jia, D. Li, S. Wang, X. Geng, F. Liu, J. Chen, S. Yang, T. P. Russell and L. Ding, *Sci. Bull.*, 2018, **63**, 340.
6. J. Yuan, Y. Zhang, L. Zhou, G. Zhang, H. L. Yip, T. K. Lau, X. Lu, C. Zhu, H. Peng, P. A. Johnson, M. Leclerc, Y. Cao, J. Ulanski, Y. Li and Y. Zou, *Joule*, 2019, **3**, 1140.